


---

**THE SPATIAL-TEMPORAL DISTRIBUTIONS OF THE TSUNAMIGENIC  
EARTHQUAKE SOURCES**

**Boris Levin<sup>1</sup>, Elena Sasorova<sup>2</sup>**

<sup>1</sup>Institute of Marine Geology and Geophysics of RAS, Yuzhno-Sakhalinsk-693022, Russia

<sup>2</sup>Shirshov Institute of Oceanology of RAS, Moscow- 117991, Russia

**ABSTRACT**

The spatial-temporal periodicity and occurrence of tsunamigenic earthquakes continue to be one of the still unsolved fundamental problems that also may have great practical operational importance. Thus, for the present investigation, we used data of tsunamigenic earthquakes (TEQ) of the last 120 years. All of the TEQ events with tectonic origin and magnitude  $M \geq 7.5$ , intensity of tsunami  $I \geq 1$ , and validity of event  $V=4$ , were selected in a working catalog which was prepared on the basis of the *Expert Tsunami Data Base for the Pacific*, and the *Tsunami Event and Runup Database* of NOAA. The total number of chosen events for the study, was 99. For these events, we analyzed the spatial and spatial-temporal distributions of the TEQ density and of released energy separately for the entire Earth, the Northern and Southern hemispheres, and for several regions of the Pacific Basin (Aleutian Islands, Kuril Islands, the equatorial belt and Central America and South America). The analysis of distribution of the TEQ in time, reveals a sharp increase in activity (density of events and of released energy) in the early 20th and 21st centuries. However, the most complete benefit of the study was the determination of the two-dimensional distribution of events (in latitudes and in time). The analysis revealed periodic changes of TEQ activity in different time intervals. The intensification of tsunami activity appears to have different periodicity at various latitudinal belts. We determined that tsunami sources are located basically in three latitudinal intervals:  $40^{\circ}\text{N} - 60^{\circ}\text{N}$ ,  $15^{\circ}\text{N} - 10^{\circ}\text{S}$  and  $25^{\circ}\text{S} - 35^{\circ}\text{S}$ . The periodicity of tsunami activity varied from 10 to 50 years.

**Keywords:** *tsunamigenic earthquake, spatial-temporal periodicity, two-dimensional distribution of events.*

## 1. INTRODUCTION

The spatial-temporal periodicity of the occurrence of tsunamigenic earthquakes continues to be one of the unsolved fundamental problems that may have great practical importance. It is known that the Earth's seismic activity demonstrates a distinct unevenness (irregularity) in both space and time. The periods of the seismic activity (SA) increases are followed by periods of decreases. These periods manifest themselves differently at different regions of the Earth. An increase of seismic activity in one region may correspond to a decrease in another region.

The objective of the present study was to examine the spatial-temporal distributions of tsunamigenic earthquakes sources. Specifically, we considered only tectonic tsunamis (caused by strong earthquakes). Such tsunamigenic earthquakes tend to have a magnitude ( $M$ ) which is greater than or equal to 7.5. Therefore to analyze the spatial and temporal distributions of tsunamigenic earthquakes (TEQ) we had to use sufficiently long series of reliable observational data. For that reason we chose to study the TEQ over the last 118 years (from 1895 to 1913). Furthermore considered were only tectonic tsunamis in which the intensity ( $I$ ) of tsunami waves was greater or equal than one. We chose the value  $I \geq 1$ , since until 1950 there was not enough reliable observations of weaker events for the Pacific. We analyzed the spatial and spatial-temporal distributions of the TEQ density and released energy separately for the entire Earth, for the Northern and Southern hemispheres, and for several regions of the Pacific Basin (Aleutian Islands, Kuril Islands, the equatorial belt, Central America, and South America).

## 2. SELECTION OF OBSERVATIONAL DATA, AND PREPROCESSING

The working catalog of tsunamigenic earthquakes was prepared on the basis of the Expert Tsunami Data Base for the Pacific (HTDB/WLD 2010), and the Tsunami Event and Runup Database at NOAA (NGDC/NOAA 2010). To analyze the spatial and temporal distributions of tsunamigenic earthquakes (TEQ) we had to use sufficiently long series of reliable observational data. Therefore we studied TEQs of the last 118 years (from 1895 to 1913).

We took into account that from 1900 to 1963 the errors in the determination of earthquake magnitude was  $\pm 1$ , the error in determining the intensity of tsunami waves ( $I$ ) for HTDB / WLD was equal to  $\pm 0.2$ , and for weak tsunamis with  $-4 \leq I \leq 0$  error was  $\pm 1$ . (Gusiakov 2011). This was the reason why we chose to study all TEQ of tectonic origin, with magnitude  $M \geq 7.5$ , intensity of tsunami  $I \geq 1$ , and event validity  $V=4$ .

Then, after removing duplicates, cross-checking and verifying the data from both databases, we selected events for the working catalog of tectonic tsunamis for which we carried out pre-processing procedures and recalculation to a single scale of magnitude values in the working directory (by conversion to  $M_s$  magnitude). This processing left 99 seismic events which were identified as sources of tectonically-generated tsunamis with intensities equal to or greater than 1.0. These events formed the basis of the working catalog for future research as well (hereafter called simply as a catalog or CTEQ).

In order to compare the spatial and spatial-temporal distributions of the TEQ and earthquakes (EQ) with  $M \geq 7.5$  were used from the working catalog of strong earthquakes for the period 1900 to 2013 (CSEQ) and used the following two versions of the catalog of NEIC (USGS/NEIC):

1. NEIC from 1973 to 2013,
2. Catalog of the Significant Worldwide Earthquakes (2150 B.C. - 1994 A.D.), compiled by USGS/NEIC on the basis of the NOAA agency's database.

The preliminary standardization of magnitudes and removal of aftershocks (more exactly the creation of a version of the working catalog without aftershocks) was carried out for the mentioned above subsets of events. The current version of the EQ catalog includes data on 620 strong global earthquakes over the past 113 years, i.e. almost since the beginning of instrumental seismic observations.

Subsequently, the temporal EQ distributions were calculated separately for eighteen latitudinal intervals (belts):  $90^{\circ}$ - $80^{\circ}$ N,  $80^{\circ}$ - $70^{\circ}$ N,  $70^{\circ}$ - $60^{\circ}$ N,  $60^{\circ}$ - $50^{\circ}$ N and so on (the size of each belt being equal to  $10^{\circ}$ ). In both cases (for TEQ and for strong EQ) the entire range of observations was subdivided into several 5-year intervals. The total number of events and the total energy released by EQ were determined in each five-year interval.

Given the fact that earthquakes occur primarily along tectonic plate boundaries, the earthquake number and the released energy values were normalized by the length of the lithospheric plate boundaries in each chosen interval of latitude. Thus we obtained the density of seismic events and the density of released energy. These values gave us the average number of earthquakes generated for every 100 kilometers of the plate boundaries and the average value of the released energy by earthquakes (i.e. capability of this section of the tectonic boundary). These characteristics have a clear physical meaning, because they allowed us to compare the seismic activity of various parts of the globe.

Thus, we analyzed the spatial and spatial-temporal distributions of the TEQ density and released energy separately for the entire Earth, for the Northern hemisphere, for the Southern hemisphere and for several regions of the Pacific Basin (Aleutian Islands, Kuril Islands, the equatorial belt, Central America, and South America).

### **3. THE SPATIAL DISTRIBUTIONS OF THE EPICENTERS OF THE TSUNAMI EARTHQUAKES AND EPICENTERS OF THE EARTHQUAKES WITH $M \geq 7.5$**

Figure 1 shows the distribution of epicenters for TEQs, which are listed in the catalog (CTEQ) on the map of the World Ocean, while Fig. 2 presents the location of the epicenters of strong EQs with  $M \geq 7.5$ , which are included in the other catalog (CSEQ). The total number of events located outside the Pacific amounts to 8 (i.e. 8% of the total number of events).

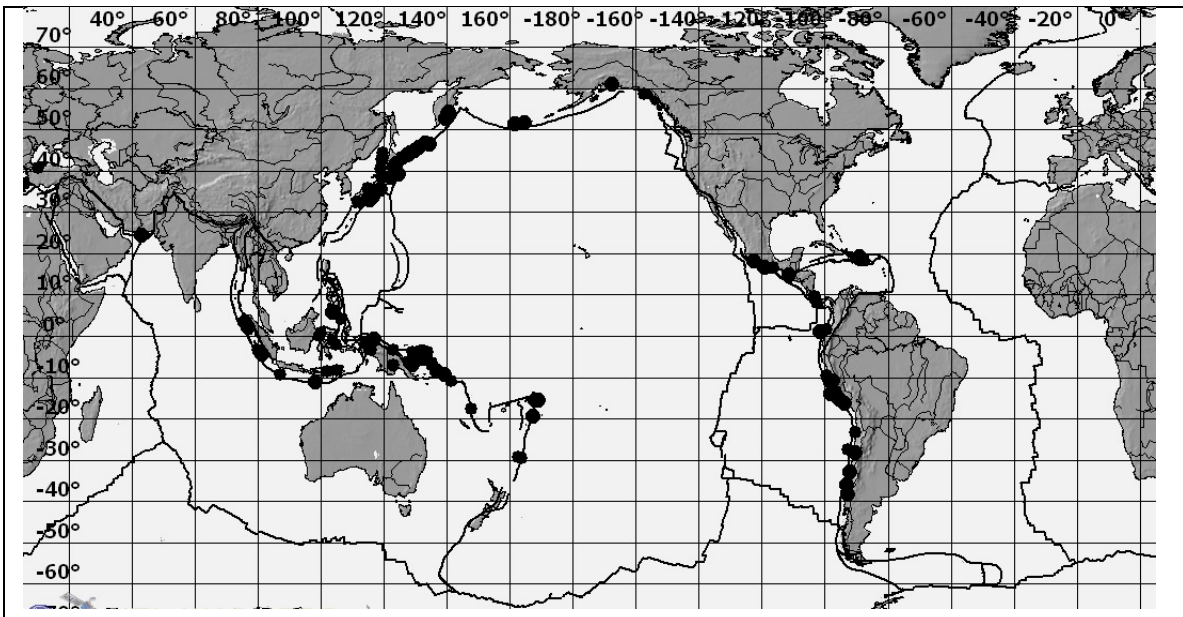


Figure 1. The distribution of the TEQ epicenters since 1895 on the world map. The epicenters are marked by black circles.

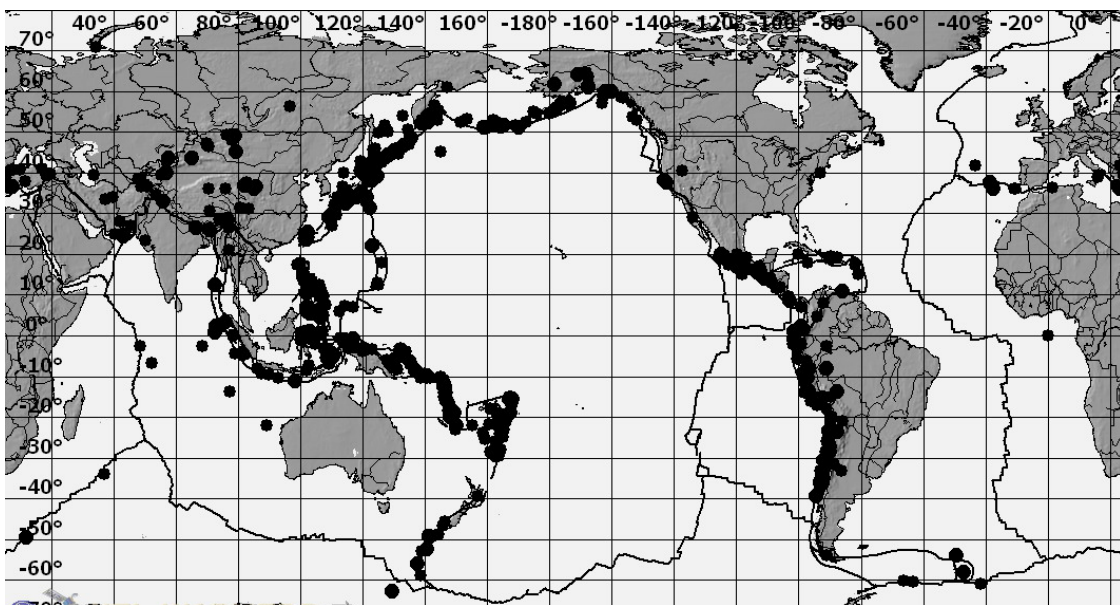


Figure 2. The distribution of the EQ with  $M \geq 7.5$  since 1895 on the world map. The epicenters are marked by black circles. The total number of the EQ amounts to 621

Analysis of the spatial distributions of the TEQ, as noted above, was based on the separation of the Earth's surface by 18 latitudinal belts (the size of latitudinal belt being equal to 10°). Fig. 3a shows the distribution of the TEQ number by latitude. On this distribution, clearly distinguished are two maxima at latitudes 40° - 50°N and 0° - 10°S, a local minimum in the vicinity of 20° - 30°N and practically zero values on the polar caps and in the high latitudes.

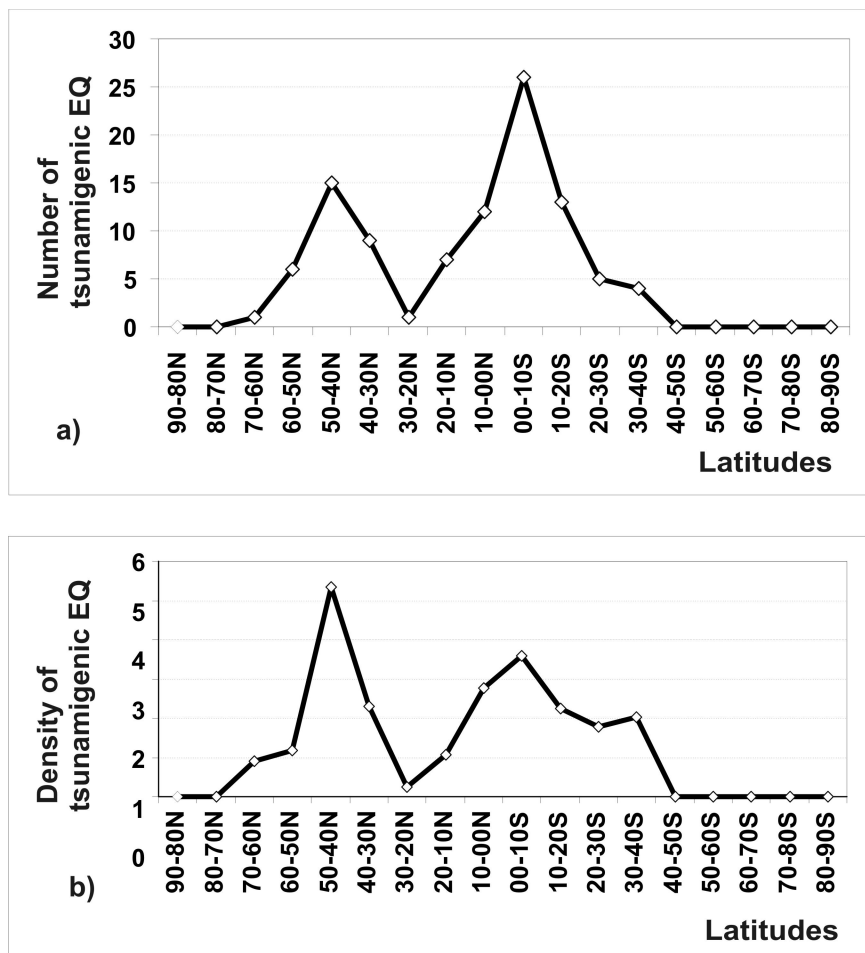


Figure 3. Latitudinal distribution of the TEQ number - (a) and the distribution of the TEQ density - (b).

The latitudinal distribution of the TEQ density is presented in Figure 3a. Basically, the distribution in Figure 3b is similar to the distribution in Figure 3a. However, the maximum in the Northern Hemisphere is marked sharper, and in the Southern hemisphere maximum in the 0° - 10°S splits into two peaks: 0° - 10°S and 30° - 40°S. The second maximum in the graph is less pronounced.

Boundaries of lithospheric plates in the northern hemisphere at latitudes 50° - 35°N and in the southern hemisphere at latitudes 10° - 40°S are located close to the meridian direction, and plate boundaries at latitudes 10°N - 20°S are mostly located in latitudinal direction. Accordingly, the total length of the plate boundaries in latitudinal belt 10° - 10°S is from 2 to 3 times more than in latitudes

40° - 50°N and 30° - 20°S, which reduces the density of the TEQ in latitudes 10°S - 10°N. That is why the maximum in the Southern Hemisphere (0° -10°S) becomes not so sharp after normalization.

Figure 1 shows the location of the TEQ epicenters on the map of the World Ocean. It is easy to note that the main TEQ occur in the Pacific region. It is possible to confidently identify spatial clusters, which are located at latitudes 55° -35°N in the western part of the northern hemisphere, at latitudes 20° -40°S in the eastern part of the southern hemisphere; and events in the latitudes 10°N - 20°S which are located in both the western and eastern parts of the Pacific.

The distribution of the strong EQ number with  $M \geq 7.5$  prepared on the basis of the working catalog CSEQ is presented in Figure 4. Also, clearly distinguished in this distribution are two maxima at latitudes 40° - 30°N and 0° - 20°S, a local minimum in the vicinity of 20° - 30°N and practically zero values on the polar caps and in the high latitudes. Thus the latitudinal distributions of the EQ number and TEQ number (Figure 3a and Figure 4) may be considered as being similar.

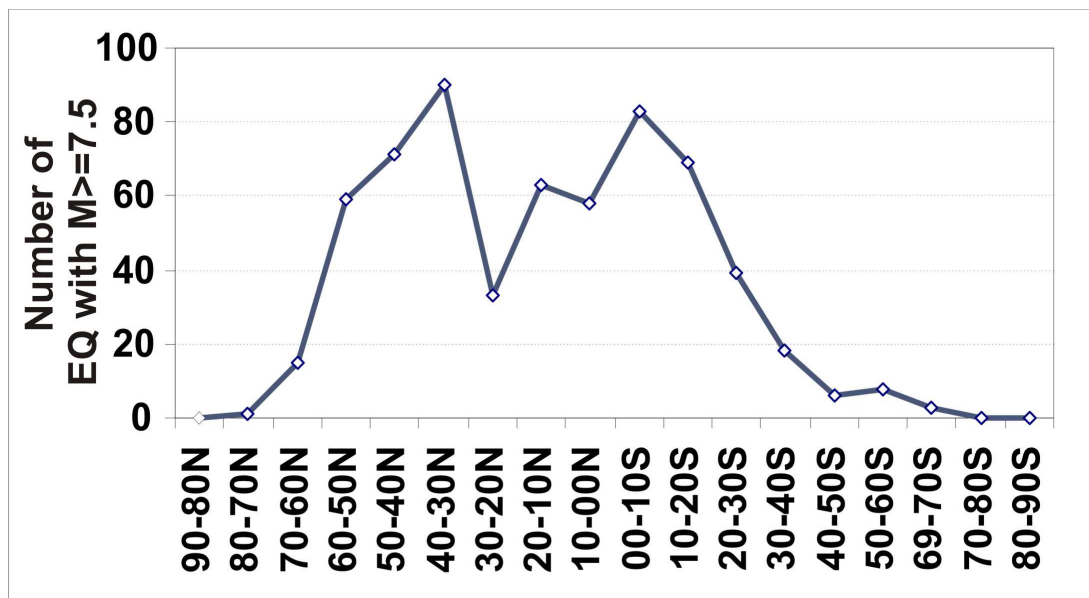


Figure 4. The distribution of the EQ number by latitude (621 events with  $M \geq 7.5$ ). The period of observation is 123 years (from 1890 up to date).

Next, we considered the latitudinal distribution of the energy released from the TEQ (Figure 5a) and energy density (Figure 5b).

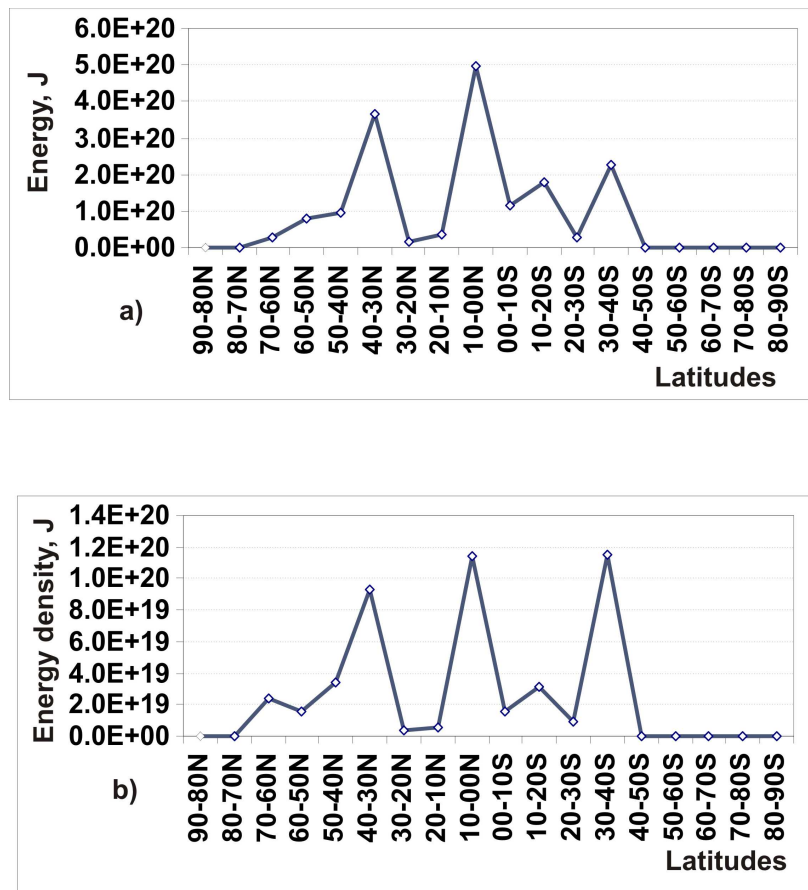


Figure 5. Latitudinal distribution of the energy released by tsunamigenic EQ – a) and the distribution of the energy density – b).

The energy released by TEQ in the latitude interval 70°N -40°S varies in range from  $2.5 \cdot 10^{19}$  to  $5 \cdot 10^{20}$ , but for the latitudes 90° - 80°N and 40° - 90°S it is equal to 0.

Furthermore, we see a distribution with three clearly distinguished local maxima: at 40° - 30°N, 10° -0°N and at 30° - 40°S; local minima between them and almost zero values of energy (and energy density) on the polar caps and in the high latitudes. Peaks at latitudes 40° - 30°N and 30° - 40°S for the energy density (Figure 5b) are sharper than in Figure 5a (for released energy) as well as in Figure 3a and 3b (for the number of events and their density). About 65.8% of the total energy is released in three latitudinal belts, corresponding to the local maxima (from 18). And about 22% of the energy is released in the latitudinal belt 40° - 30°N, at latitudes 10° - 00°N the energy released amounts to 29.9%, and at latitudes 30° - 40°S to 13.7%.

The energy distributions of the TEQ presented above differ significantly from the latitudinal distributions energy density of earthquakes (Figure 6b) which have a pronounced bimodal shape with two maxima at latitudes 30° - 40°N and 20° -30°S (Sasorova et al. 2013). The distributions in Figure 6 were obtained on the basis of International Seismological Catalogue: (ISC) for more than 200000 events with  $M \geq 4.0$  (data from 1964 up to date).

Both plots have a distinctly bimodal shape and location of peaks of seismic activity, being the same in the Northern and in the Southern hemispheres. Figure 6 was adopted from the work of Sasorova (Sasorova et al. 2013).

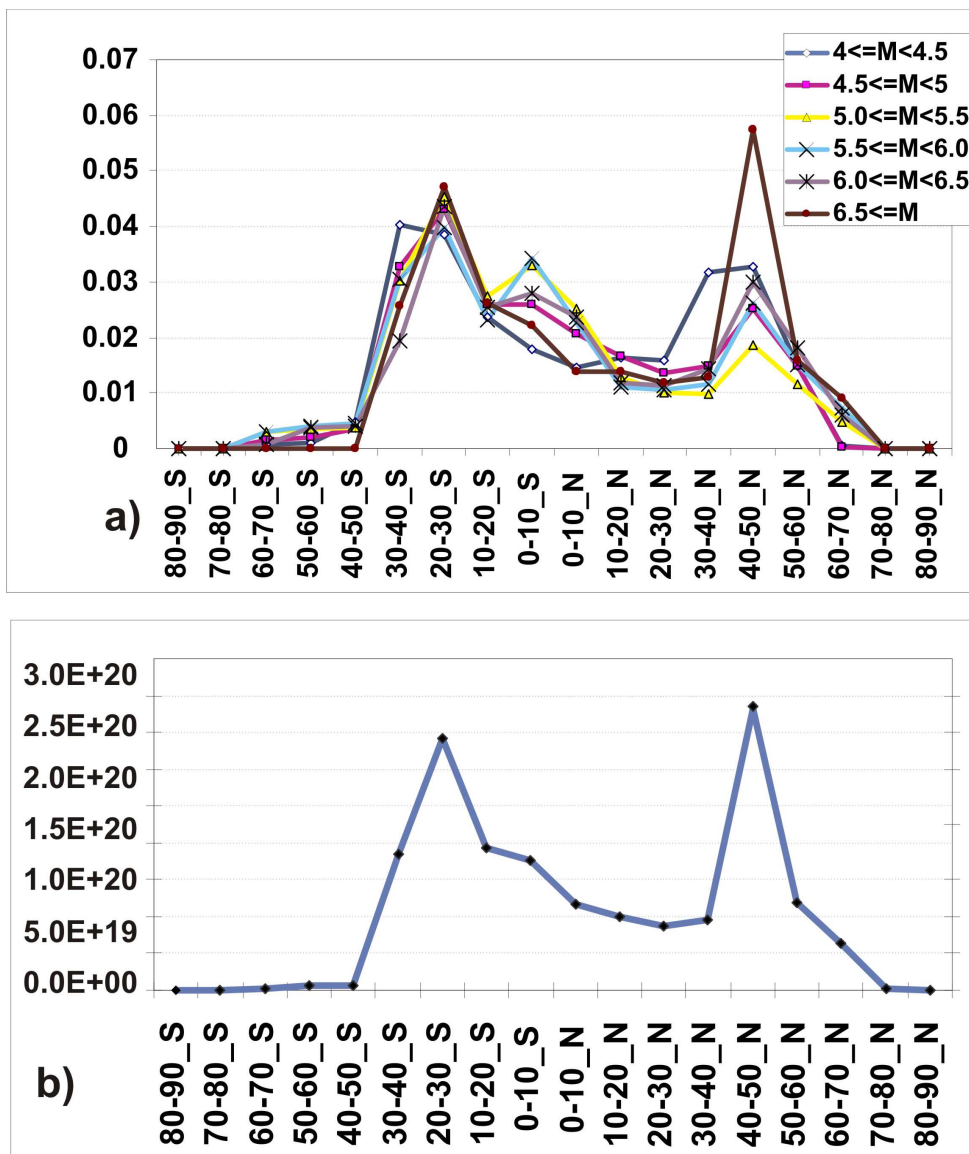


Figure 6. Distributions of the relative seismic event density by latitudes for 6 magnitude ranges – a) and the distribution of the energy density by latitudes – b).

#### 4. THE TEMPORAL DISTRIBUTIONS OF THE TSUNAMIGENIC EQ EPICENTERS

The distributions of the TEQ density per five-year interval are shown in Figure 7: a) - for the whole Earth, b) - for the Northern Hemisphere and c) - for the Southern Hemisphere. The vertical

axes scale kept constant for all three fragments. The horizontal axes of all fragments are indicated upper limits of each five-year interval.

In Figure 7, we can observe the periodic increase and decrease of the event density in time, and the noticeable asymmetry of the increasing and decreasing of the activity TEQ for the Northern Hemisphere and for the Southern Hemisphere.

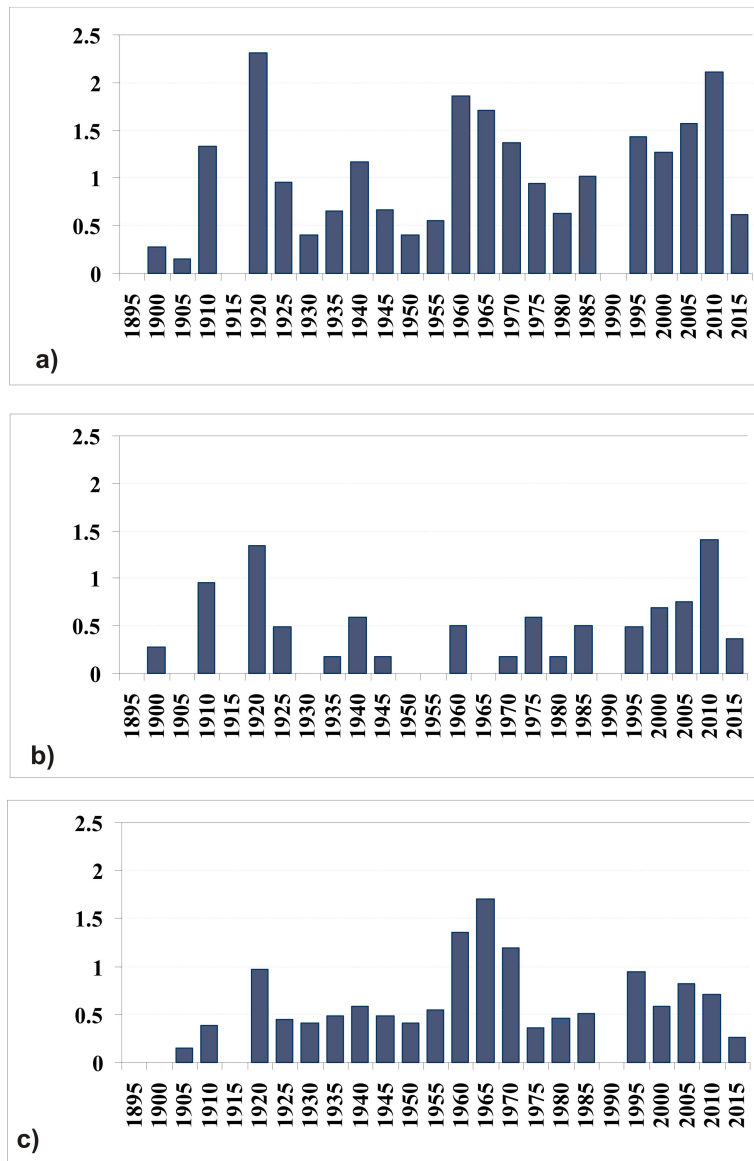


Figure 7. The distributions of the TEQ density per five-year interval: a) - for the whole Earth, b) - for the Northern Hemisphere and c) - for the Southern Hemisphere. The vertical axes are density of the TEQ. The labels on the horizontal axes correspond to upper limit of each five-year interval.

The distributions of the energy density released by TEQ per five-year interval are shown in Figure 8: a) - for the whole Earth, b) - for the Northern Hemisphere and c) - for the Southern Hemisphere.

The most powerful TEQ's occurred at the beginning of the 21st century. They occur in both the Northern and Southern Hemispheres, but in different five-year intervals.

Weaker peaks of the tsunami activity (by value of the released energy) occurred at the beginning of the 20th century and the middle of it (1950-1965). Also, detected was the periodicity of occurrence of the TEQ within the considered time period.

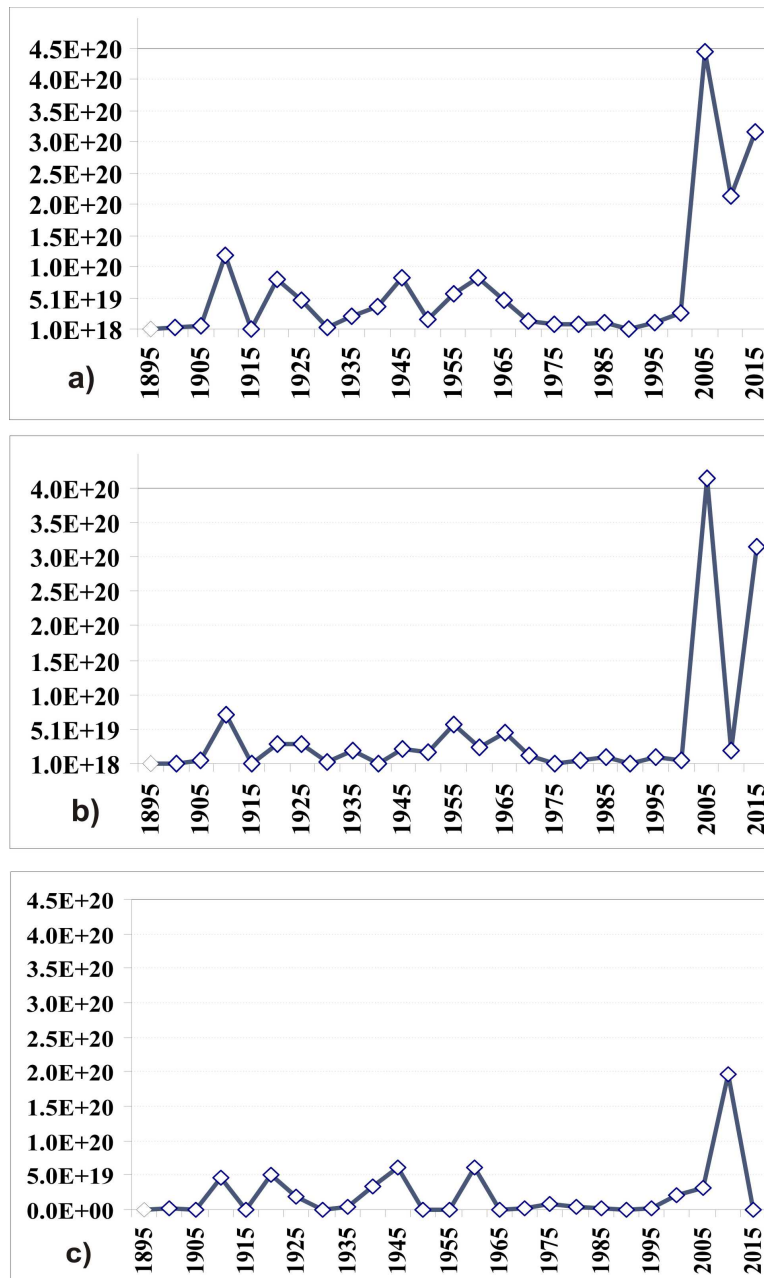


Figure 8. The distributions of the energy density per five-year interval: a) - for the whole Earth, b) - for the Northern Hemisphere and c) - for the Southern Hemisphere. The vertical axes are energy density. The labels on the horizontal axes correspond to upper limit of each five-year interval.

The increase of the TEQ activity appears sequentially in the Northern Hemisphere, and then in the Southern Hemisphere (and vice versa) as shown in Figure 9. The vertical axis indicates the total amount of energy released from these earthquakes. That part of the energy that released in the Northern Hemisphere is shown in blue, and that part of the energy which falls on the Southern Hemisphere is shown in red.

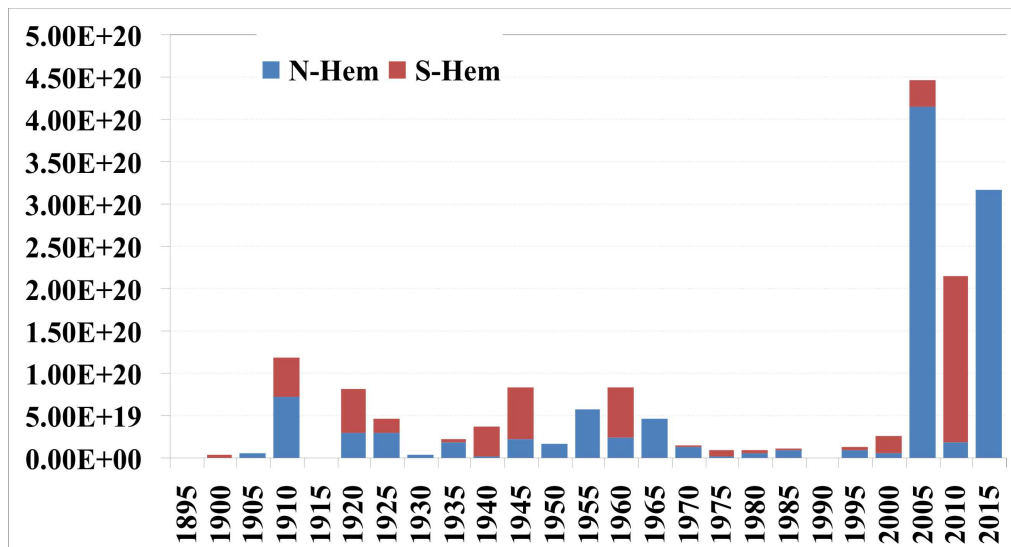


Figure 9. The total energy density distribution for the two hemispheres (red color is the part of the energy released in the Southern Hemisphere, and the blue color is the energy released in the Northern Hemisphere).

For example, the time intervals 1940, 1945 are marked generally in red (events in the Southern Hemisphere), but two following intervals (1950, 1955) are marked as blue (events in the Northern Hemisphere). Let us also consider three more powerful TEQ in the beginning of the 21 century: Indonesian Tsunami of 26.12.2004 (Northern Hemisphere), the Chilean Tsunami of 27.02.2010 (Southern Hemisphere), and subsequently, the Tohoku Tsunami of 11.03.211 (Northern Hemisphere). This feature of the sequential occurrences of strong earthquakes in different hemispheres was noted earlier in (Levin and Sasorova 2005, Sasorova et al. 2006), and for tsunamigenic earthquakes in other works (Levin and Sasorova 2002, Sassorova and Levin 2004).

Subsequently, let us compare the temporal distributions of the EQ number (with  $M \geq 7.5$ ) in Figure 10 and the temporal distributions of the TEQ number in Figure 7. Noteworthy in Figure 10 is the observed pronounced increase and decay of seismic activity within a period about 30 years. This periodicity for the TEQ (Figure 7) is expressly much weaker.

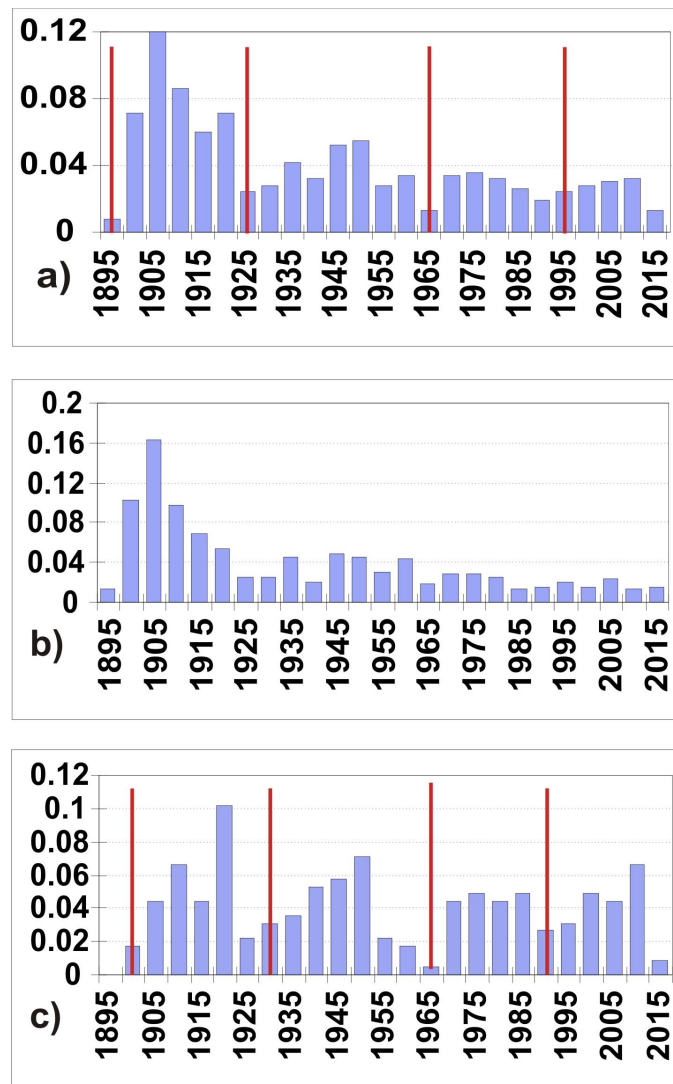


Figure 10. The distributions of the relative number of the EQ with  $M \geq 7.5$  per five-year interval: a) - for the whole Earth, b) - for the Northern Hemisphere and c) - for the Southern Hemisphere. The labels on the horizontal axes correspond to upper limit of each five-year interval

Subsequently we compared the temporal distributions of the energy released by EQ (with  $M \geq 7.5$ ) in the Figure 11 and the temporal distributions energy released by the TEQ (Figure 8.)

The peaks of released energy in Figure 11 are observed in the early 20th and 21st centuries in all three fragments. The peaks of energy at the beginning of the 21st-century were generated due to a series of megaequakes EQ. The maxima of the energy released at the beginning of the 20-century can be explained, because of the fact that in this five-year intervals several EQ with  $M \geq 8.0$  occurred (from 6 to 10 events per two year period). Also, it can be observed that two local maxima occurred in the Northern Hemisphere for the periods 1930 - 1950 and from 1950 - 1970; and two local maxima in the Southern Hemisphere: for the periods 1935 - 1955, and 1970 - 1990.

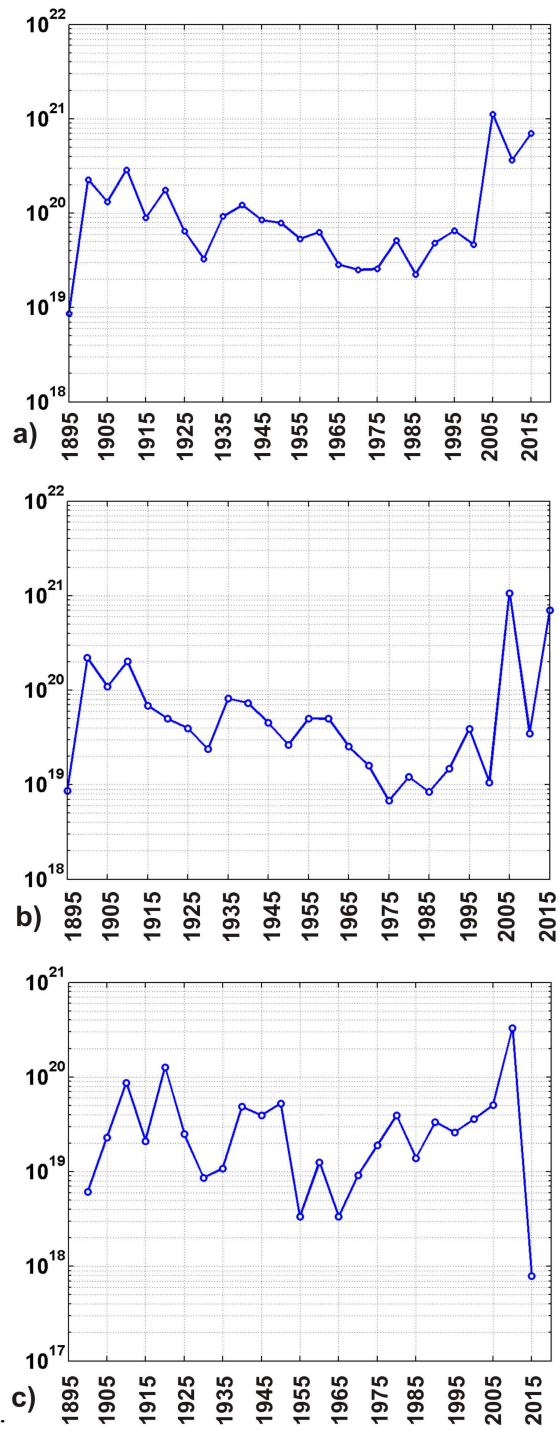


Figure 11. The temporal distributions of the energy density released by strong EQ with  $M \geq 7.5$  per five-year interval for: a) - for the whole Earth, b) - for the Northern Hemisphere and c) - for the Southern Hemisphere. The vertical axes are energy density in J (logarithmic scale). The labels on the horizontal axes correspond to upper limit of each five-year interval.

## 5. SPATIAL-TEMPORAL DISTRIBUTIONS OF THE TEQ DENSITY AND RELEASED ENERGY

In the previous sections we discussed separately the latitudinal and temporal distributions of both density of the number of TEQ and the density of energy released from these events. However, the most complete picture gives two-dimensional, space-time, distribution of events. This representation technique of the distributions of seismic activity was used previously by the authors (Levin and Sasorova 2010, Sasorova et al. 2013).

The two-dimensional distribution of the TEQ density (Figure 12) shows that this representation identifies areas in which for more than a hundred years any tsunamigenic EQ (polar caps and high latitudes) did not occur. However, the situation is different for the Southern hemisphere since it comprises a much more extended zone, extending from 40°S up to the South Pole. The same holds true for the Northern hemisphere since this area starts from 70°N. It is interesting to note that the area with very weak tsunami EQ activity (practically zero-order) was observed in the latitude belt 30° - 20°N.

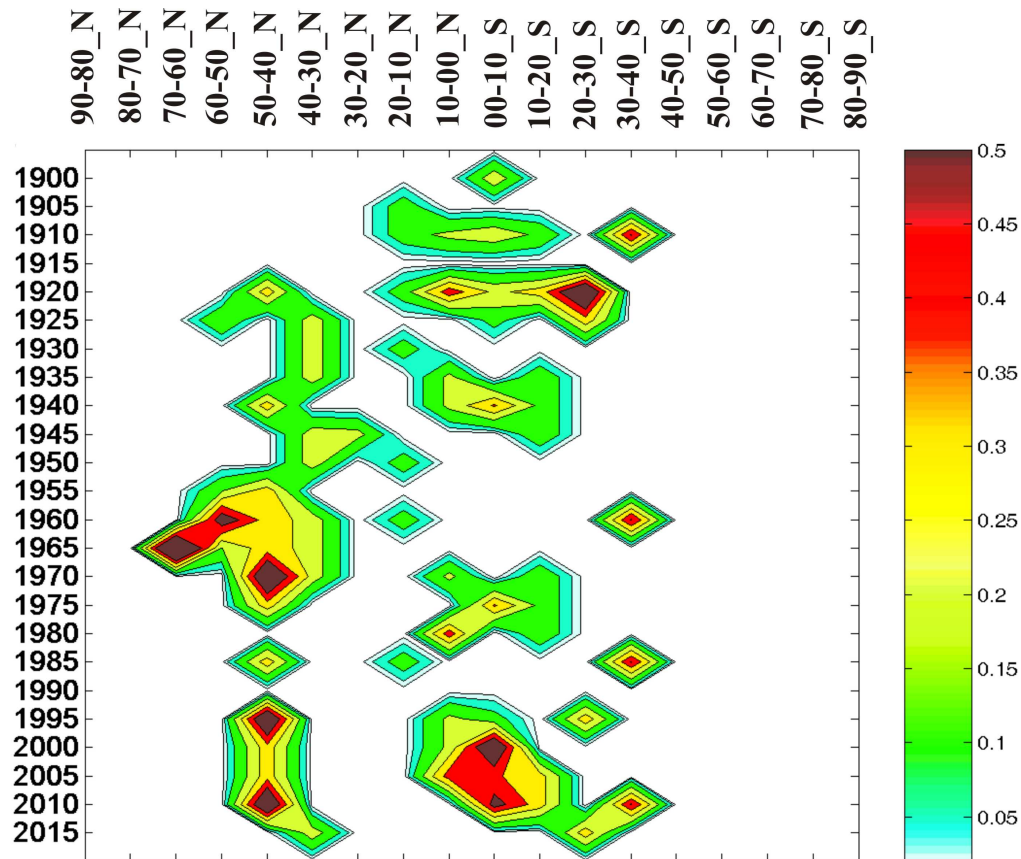


Figure 12. Two-dimensional distribution of the TEQ density by latitude and time from 1985 to 2013. The labels on the vertical axis correspond to upper limit of each five-year interval along the horizontal axis - latitudinal belts. The color scale on the right side of the figure corresponds to the density of events.

The occurrence periodicity of tsunamigenic earthquakes is clearly shown in Figure 12. The periods of TEQ activity intensification are not coinciding at different latitudinal zones. In the Northern Hemisphere peaks of activity of several large events can be observed at a comparatively short time intervals. Specifically, such peaks of activity occurred in the middle of the 20th century from 1955 to 1975, then after a 20-year interruption, by subsequent events from 1990 to 2010. There are also two, less powerful clusters in the time intervals from 1915 to 1920 and from 1980 -1985.

In the equatorial region peaks tsunami activity are observed at intervals of 25 years (in the first half of the 20th century), then at intervals of 30-40 years (mid-century), and again at intervals of 25 years to the end of the 20th century. In the Southern Hemisphere almost identical peaks of the tsunami activity are observed at intervals of 50 years in the first half of the 20th century, thereafter at intervals of 25 years from 1960 up to date.

Figure 13 shows a two-dimensional distribution of the energy density released by the TEQ. This distribution is generally identical to the distribution in Figure 12. The color scale on the right side of the figure gives the value of the released energy  $E = 10^N$  in J. The two-dimensional distribution of the energy density almost coincides with the two-dimensional distribution of the density events.

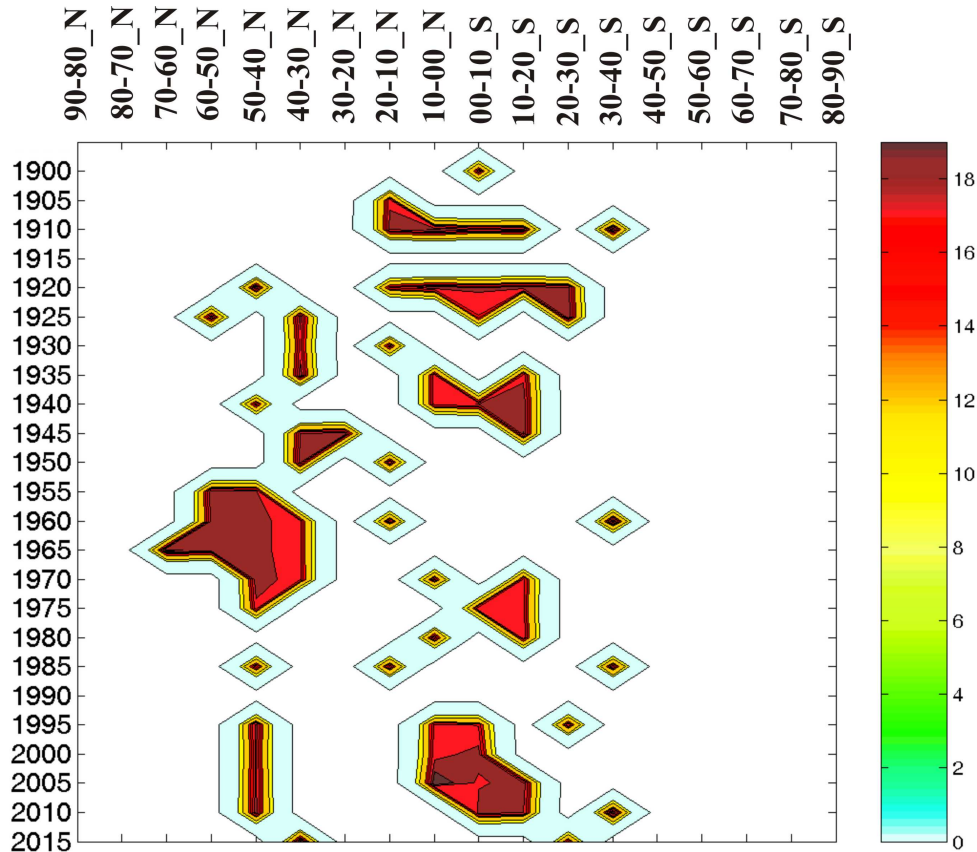


Figure 13. Two-dimensional distribution (by latitude and by time) of the energy density for the TEQ from 1985 to 2013. Legends of all axes are the same as in Figure 12.

## 6. PECULIARITIES OF THE DISTRIBUTION OF THE TEQ SOURCES IN THE PACIFIC REGIONS

Let us now consider the spatial-temporal distributions of the TEQ sources in the following sub regions: Kuril-Kamchatka, Japan area, South America, Central America and the equatorial zones, as well as the periodicity of manifestation of tsunamigenic earthquakes in the regional distributions.

The spatial-temporal distribution of the TEQ epicenters for the Kuril-Kamchatka zone is shown in Figure 14. It may be noted that no tsunamigenic earthquakes are observed in the latitude belt from 47°N to 51°N, in the time interval from 1900 to 2013. However, there is a coincidence in the appearance of the TEQ in Kamchatka and the Kuril Islands in certain time intervals from 1915 to 1920 and from 1950 to 1960, and in the periodicity of tsunami occurrence with periods of 20 to 35 years.

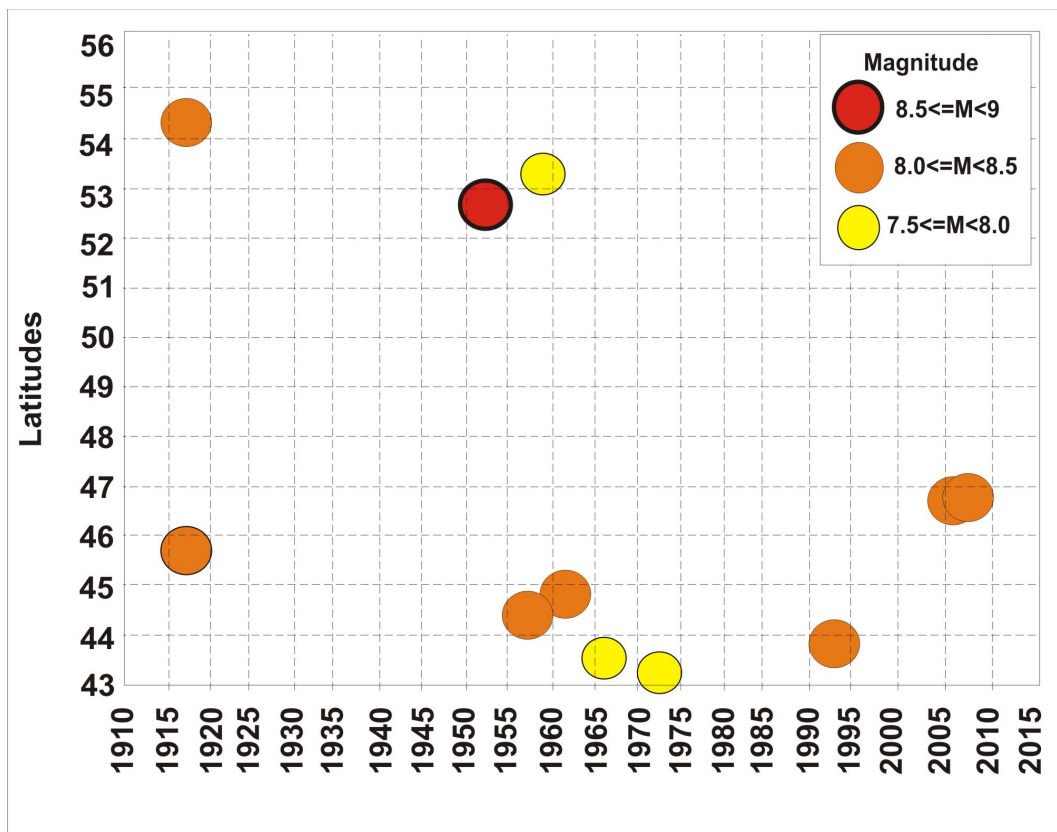


Figure 14. The two dimensional distribution of the TEQ in the Kuril-Kamchatka region (by latitudes and by five-year interval). The vertical axis represents latitudes of the TEQ epicenter. The labels on the horizontal axis correspond to the upper limit of each five-year interval. The magnitude legend is in upper-right corner.

The spatial-temporal distribution of the TEQ epicenters for the Japan zone is presented in two fragment of Figure 15 (15a – the Pacific part of Japan and 15b - the Japan sea).

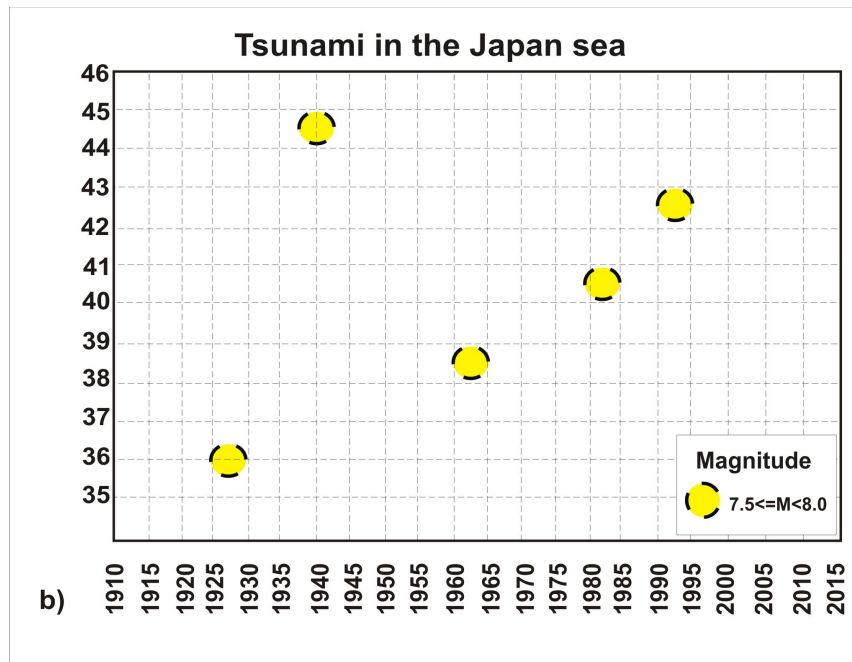
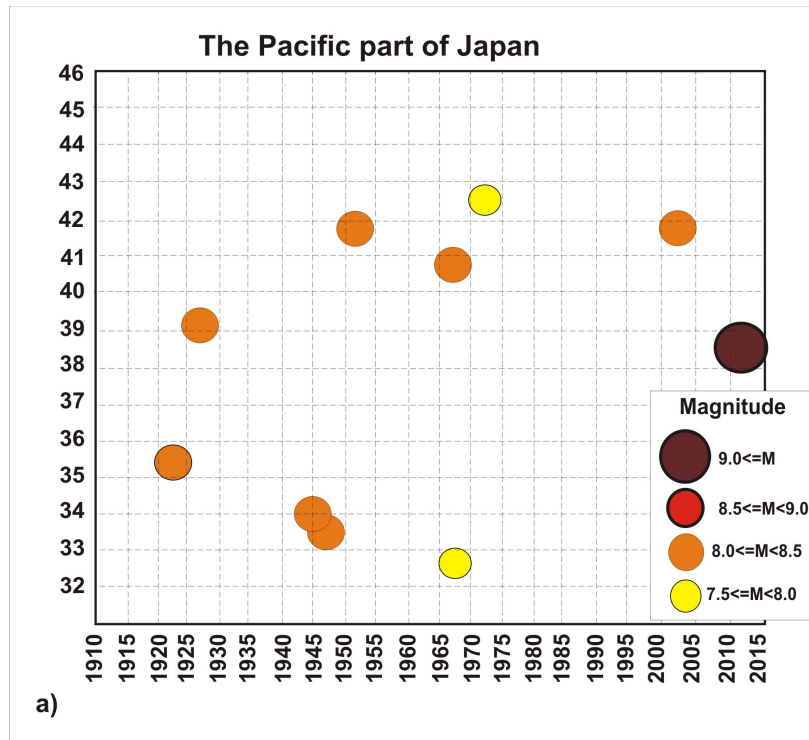


Figure 15. The two-dimensional distributions of the TEQ (per latitudes and five-year interval): a) - in the Pacific part of Japan, b) in the Sea of Japan. The vertical axes are the latitudes of the TEQ epicenter. The labels on the horizontal axes correspond to the upper limit of each five-year interval. The magnitude legend is in bottom-right corner of each plot.

The latitudinal belt from 34°N to 40°N in Figure 15a may be discriminated, where from 1930 to 2010 strong tsunamigenic earthquake epicenters were not observed. The periodicity of the intensifying tsunami activity with periods 20 - 25 years may be marked. In the latitude belt 38°N - 45°N (Figure 15b, Sea of Japan) a migration of the TEQ epicenters is noted from south to north in the period (1960-1995) with a periodicity of about 20 years. All epicenters of tsunamigenic earthquakes in this latitude belt, locate almost on the same longitude (139.09°E to 139.53°E).

The spatio-temporal distribution of the TEQ epicenters in South America (Pacific Coast) is shown in Figure 16.

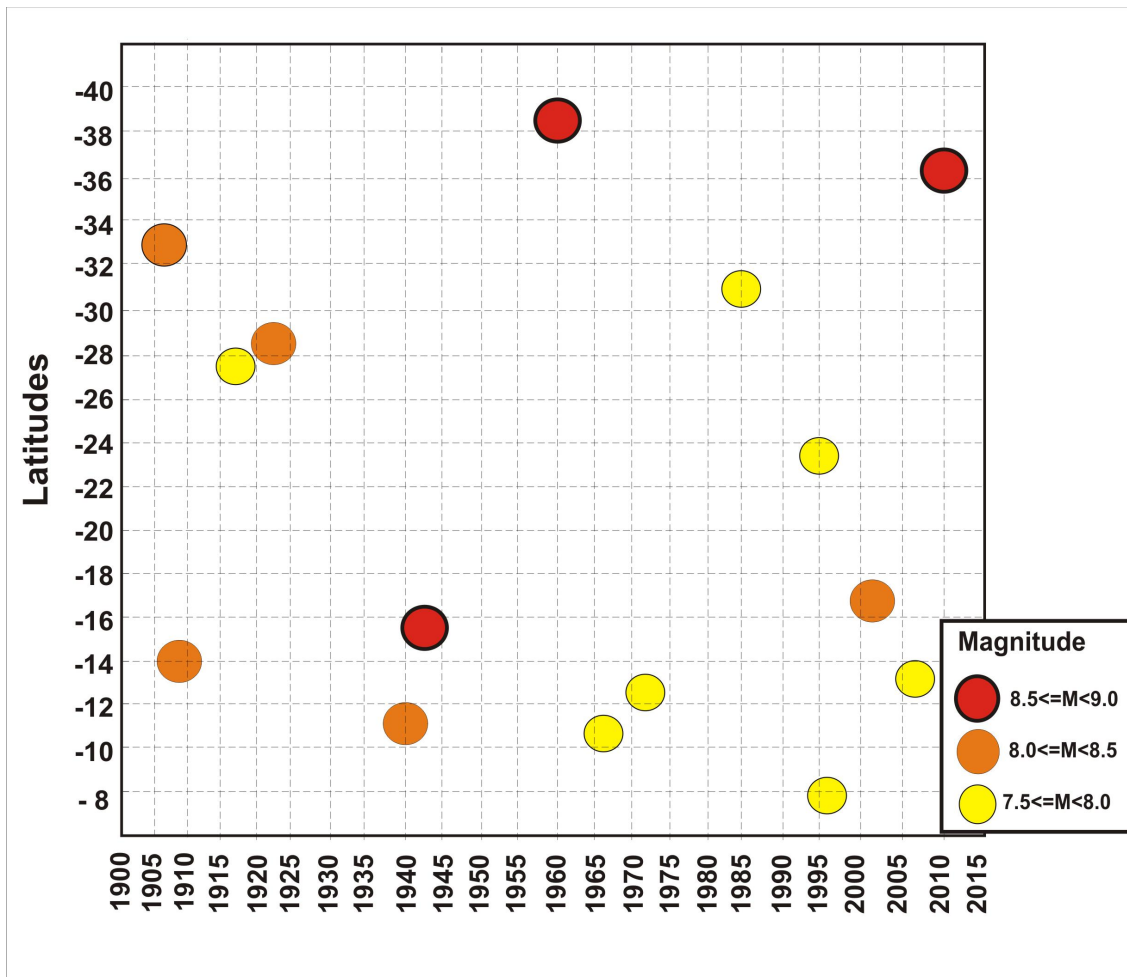


Figure 16. The two-dimensional distributions of the TEQ (by latitudes and by five-year interval). The vertical axis shows the latitudes of the TEQ epicenters. The labels on the horizontal axis correspond to the upper limit of each five-year interval. The magnitude legend is in bottom-right corner of the plot.

An analysis of figure 16 allows us to mark:

- the existence of two latitudinal belts from 8°S to 18°S and from 26°S to 40°S, where almost all the epicenters of the TEQ are located.
- the latitude interval which display weak tsunami activity ranges from 18°S - 26°S.

The frequencies of occurrence of tsunamigenic earthquakes in active zones are different and range from 25-30 years for zone 8°S - 18°S and from 45-50 years for the belt 26°S - 40°S. These periodicities may be observed before where we analyze Fig. 12 and Fig. 13. Periods of activation in the zone of 26°S - 40°S correspond mainly to periods of activity decrease in the zone of 8°S - 18°S.

The spatio-temporal distribution of TEQ epicenters for Central America (Pacific Coast and Caribbean region) is given in Figure 17.

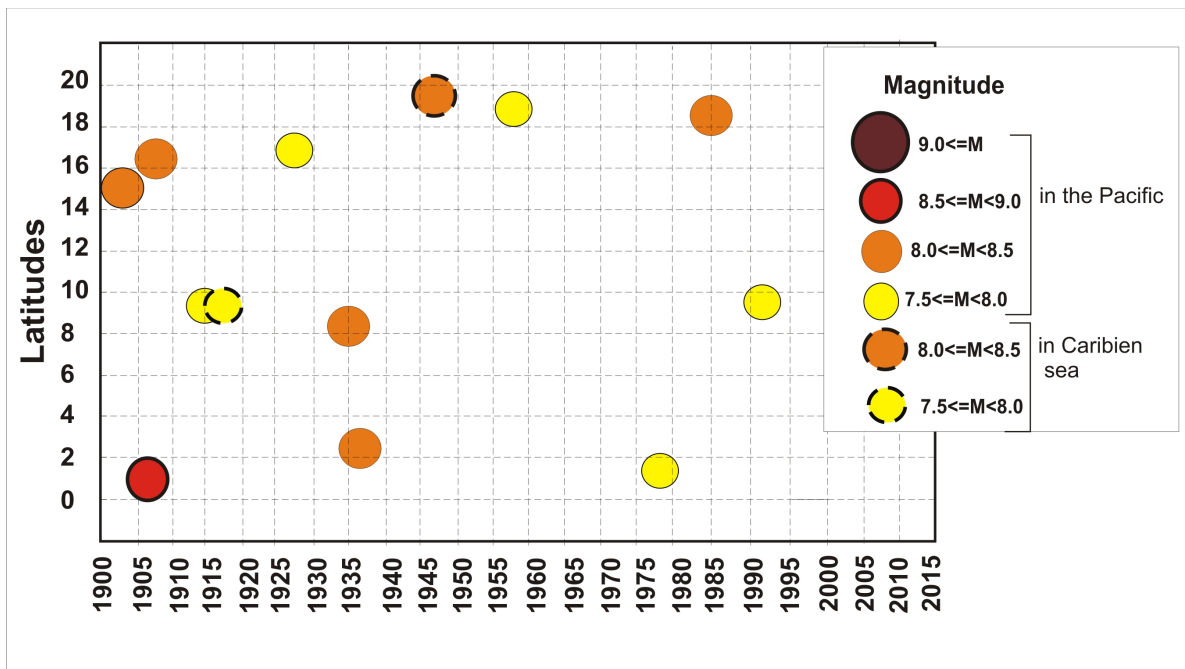


Figure 17. The two-dimensional distributions of the TEQ (per latitudes and per five-year interval). The vertical axis is the latitudes of the TEQ epicenter. The label on the horizontal axes corresponds to upper limit of each five-year interval. Legend for magnitude is in upper-right corner of the plot.

The spatial differentiation of the location of the TEQ epicenters in this figure is not expressed adequately. However a periodicity of 30-35 years for the TEQ sources located in the Pacific Ocean can be seen. After 1991, no significant tsunamis in this region were observed.

The spatio-temporal distribution of TEQ epicenters for the subequatorial region of the Pacific is given in Figure 18.

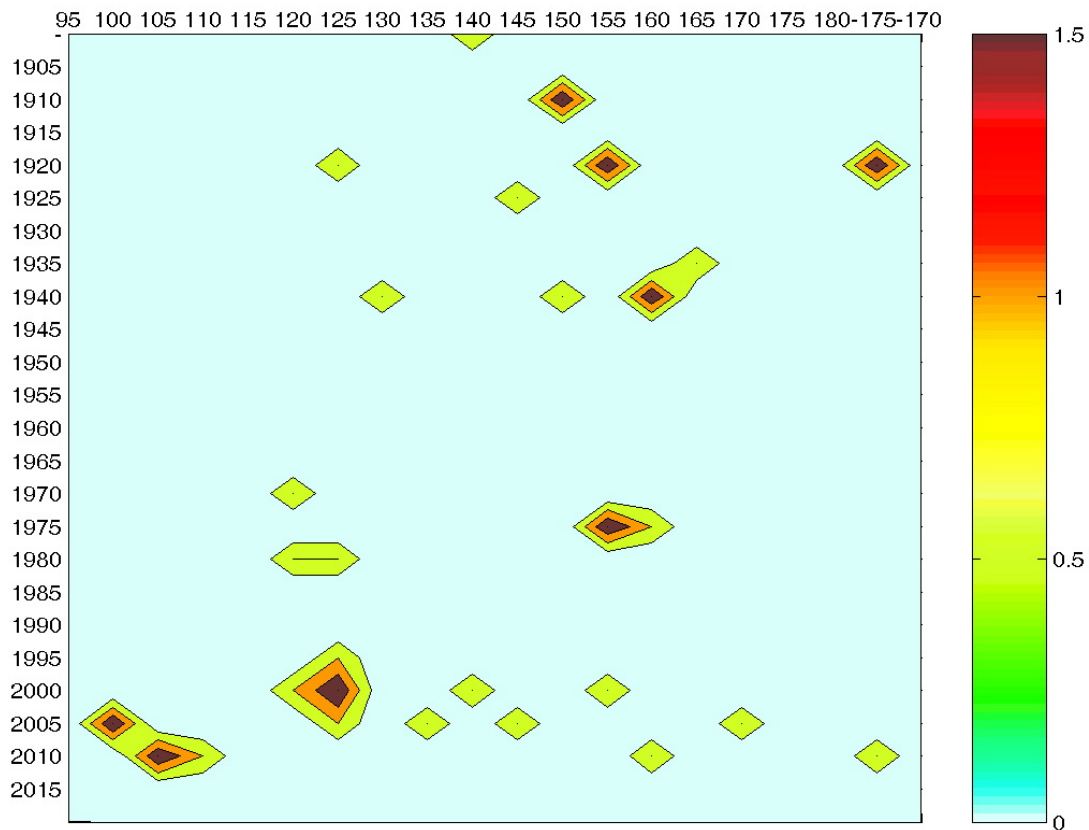


Figure 18. The two-dimensional distributions of the TEQ (by longitudes and by five-year interval). The horizontal axis is the longitudes. The labels on the vertical axis correspond to upper limit of each five-year interval. The color scale of the TEQ density is in the right corner.

This region (see Figure 1) has an extended longitudinal area with the length of the boundaries of the lithospheric plates being about 6600 km. Therefore, the two-dimensional distribution is represented here: longitude - time (in contrast to the previous figures with distributions of latitude-time).

In the region ranging from longitude 95°E to 120°E no events were observed from 1900 to 1965. Also, reduced tsunami activity is shown from 1940 to 1970. An increase in activity in the zones ranging from 115°E to 120°E and from 150°E -155°E, occurred from 1970 to 1985.

After the events of 02.07.1996 and of 29.11.1998, the tsunami activity increased throughout the equatorial zone until 2004, when the catastrophic Indonesian tsunami 26.12.2004 occurred, followed by a series of events (6 tsunamigenic earthquakes). The series contain four events with epicenters located in a relatively small longitudinal zone from 97°E to 107°E (two of the four events had  $M = 8.5$ ).

The energy distributions for the selected regions are not presented here because the maximum of the distribution of the energy released by the TEQ, corresponds to the location of the strongest events

in each region. For example, these maxima in time and space correspond to the following catastrophic events: for the Kuril-Kamchatka zone - Kamchatka TEQ (4.11.1952) and two Simushir TEQ (2006 and 2007); for Japan -a catastrophic earthquake in Tohoku (11.03.2011); and for the equatorial zone - Indonesian TEQ (26.12.2004).

## 7. DISCUSSION AND CONCLUSIONS

First of all, we considered the statistical characteristics of the TEQ, which were identified taking into account the magnitude and geographical parameters of their distributions. The resulting working catalogs (CTEQ and CSEQ) allowed us to answer the question: what part of the strong EQ generates a tsunami if the magnitude threshold of a strong EQ varies from: 7.5, to 8.0, to 8.5. These data were calculated and are presented in Table 1 below.

Table 1. A comparison of the number of strong earthquakes with the number of tsunamigenic earthquakes of the same magnitude.

	<b>Events with <math>M \geq 7.5</math></b>		
	The whole Earth	Northern Hemisphere	Southern Hemisphere
Total number of the EQ	621	393	228
Number of the TEQ, with $I \geq 1$	100 (16%)	51 (13%)	49 (21%)
	<b>Events with <math>M \geq 8.0</math></b>		
Total number of the EQ	175	119	56
Number of the TEQ, with $I \geq 1$	47 (30%)	28 (24%)	19 (34%)
	<b>Events with <math>M \geq 8.5</math></b>		
Total number of the EQ	9	5	4
Number of the TEQ, with $I \geq 1$	9 (100%)	5 (100%)	4 (100%)

It is shown that the average number of the tsunamigenic earthquakes is equal to 16% for events with  $M \geq 7.5$  and near 29% - for events with  $M \geq 8.0$ . The relative number of the TEQ in the Northern Hemisphere is more than in the Southern Hemisphere for all magnitude ranges.

However, all the catastrophic EQ (with  $M \geq 8.5$ ) result to tsunami generation. The epicenters of these events are located in the Pacific (4 - in South America, 3 - in the northern part of the equatorial zone, 1 - on Kamchatka, 1 - in Japan). It should be mentioned that these features of the distributions the TEQ were reflected in previous studies [Levin and Sasorova 2002, Levin and Sasorova 2013].

Comparison of the number of the strong EQ with the number of tsunamigenic earthquakes and of the released energy to the five regions of the Pacific (for three magnitude ranges). These data were calculated and are presented in Table 2 below.

Table 2. A comparison of the number of strong earthquakes with the number of tsunamigenic earthquakes of the same magnitude for five regions.

	<b>Events with <math>M \geq 7.5</math></b>				
	Kurile-Kamchatka zone	Japan	The near-equatorial belt	The South America	The Central America
Latitudes	43°N-55°N	32°N-46°N	6.3°N-19.5°S	8.5°S-40°S	20°N-0°N
Longitudes of the regions	144°E-165°E	130°E-144.5°E	95°E-168°W	85°W-65°W	110°W-60°W
Total EQ number	43	64	124	60	67
Number of the TEQ, with $I \geq 1$ .	11 (26%)	14(22%)	38 (31%)	16 (26%)	12 (18%)
	<b>Released energy, J</b>				
Total sum	1.73E ± 20	8.71E ± 20	1.42E ± 21	4.96E ± 20	2.8E ± 20
Released by the TEQ with $I \geq 1$	1.16E ± 20 (67%)	4.00E ± 20 (46%)	5.94E ± 20 (42%)	3.8E ± 20 (76%)	1.0E ± 20 (38%)

The relative number of events with  $M \geq 7.5$  generated a tsunami and the range of magnitudes averaged over all regions increased to 24.6% (compared with 16% of the tab. 1). This may be explained by the fact that numerous events in mainland Asia are not located in Pacific regions, so the total number of EQ decreased (from 621 to 595).

However, for all regions that were examined, the amount of energy released by the TEQ averaged more than 50% (53.8%), and this ratio varies from one region to another. So in South America and the Kuril-Kamchatka zones the energy released by the TEQ is equal to 76% and 67% of the total energy, respectively, with the catastrophic EQ contributing most of the energy.

At the present time the detection of tsunami waves in the open ocean is a solvable problem. However, when the tsunami source is close to the coast, it is very difficult to issue a local tsunami warning within a 15 to 20 minutes before the first of the tsunami waves strikes, so the magnitude-geographical principle remains the dominant factor for evaluation. It is assumed that tectonic tsunamis are generated by earthquakes for which  $M \geq M_{tr}$  and that there exists a dependence of the tsunami waves' intensity (I) on the EQ magnitude:  $I=f(M)$ . The  $M_{tr}$  is the threshold value, which is chosen separately for each region.

Attention to another study (Gusiakov 2011), should be drawn, in which a detailed investigation of the intensity of the tsunami waves on the magnitude TEQ on the basis of observational data was provided – specifically for various examined observation periods (from 1900 to 2010 and from 1990 to 2010) and for different magnitude scales for the events that generated tsunamis. Attempts to find a significant correlation between the magnitude of the tsunamigenic earthquake and the intensity of the tsunami waves were not successful up to now.

A scatter chart for the observation period from 1900 to 2010 shows that for events with  $M \geq 7.5$  and  $I \geq 1$  the regression equation with an acceptable value of  $R^2$  (the value of the reliability of the approximation) was not possible. Data in this range is almost uniformly distributed within a rectangular window (Figure 19).

The  $R^2$  values we recalculated on scatter charts for linear regression on the basis of data presented in the catalogs, varied from 0.11 to 0.25, which does not suggest the presence of significant dependence  $I=f(M)$ . Using the quadratic regression dependence did not lead to a noticeable improvement in the value  $R^2$ . However, the lack of sufficiently reliable functional dependence  $I=f(M)$  leads to the appearance of false tsunami warnings.

The above listed facts suggest:

- a weak correlation between the intensity of the tsunami and the earthquake magnitude;
- a sharp decline in the share of the TEQ (16%) if the threshold of the EQ magnitude is decreased to  $M \geq 7.5$ ;
- a significant difference in the latitudinal distributions of energy for a strong EQ and TEQ;
- detection of periodicities of the tsunami occurrence in space and time;

Apparently, these lead to the conclusion that the TEQ, have a specific properties that arise in their sources, thus requiring additional research in determining the characteristics of such sources.

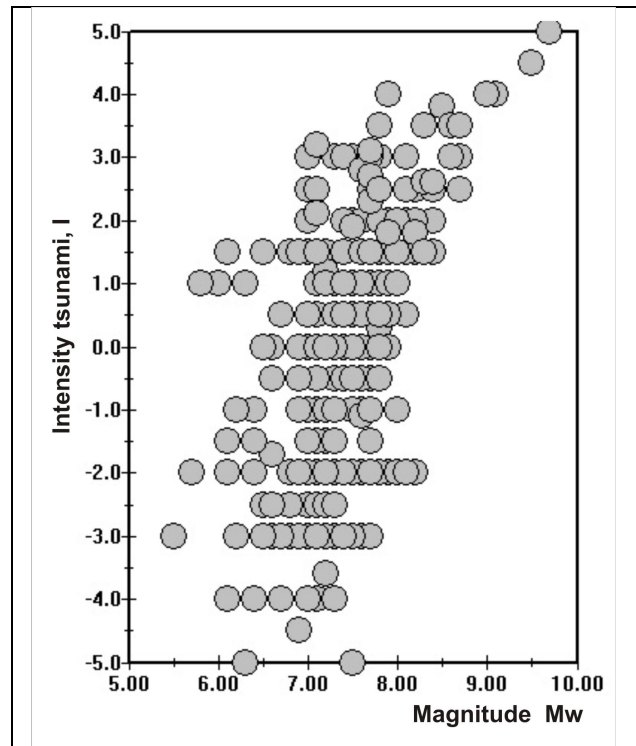


Figure 19. Scatter chart for 360 tsunamigenic events in the world's oceans from 1900 to 2010 (with  $M > 5.0$ , and  $I > -5.0$ ). Events are marked by circles gray. The intensity of the tsunami on the scale defined Soloviev-Imamura. Figure was adapted from (Gusiakov, 2011).

The focal sources for most earthquakes (98%) that generated the tsunamis shown in the CTEQ catalog had a depth of  $H \leq 60$  km. In the working directory (before preprocessing) only four events did not satisfy the above condition of focal depth (for two events the earthquake focal depth was not been determined, one having  $H = 80$  km, and the other one having  $H = 230$  km). All these events belong to the early instrumental period (until 1923), where there was a large error in the determination of earthquake focal depth.

The number of events with  $H \leq 60$  km for the EQ with  $M \geq 7.5$  is equal to 86%, about 6% of the EQ has depth  $60 \leq H < 120$  km, the depth 6% of the EQ is  $120 \leq H < 350$  km, and about 2% of the EQ have depth equal to  $H \geq 500$  km.

Analysis of Figures 12 and 13 indicates that occurrence and frequencies of tsunamigenic earthquakes is greatly affected by regional peculiarities. This may be caused by the fact that almost all sources of the TEQ in the western part of the Pacific are associated with the boundaries of compressed island arcs.

The minimum distance from the source to the coast (MD) for each tsunamigenic earthquake and the MOD values (average value of the MD values defined for all events in the region) were previously calculated (Sasorova et al. 2008) which also determined that 87% of the TEQ sources in the Pacific

basin were no further than 100 km from the closest shoreline, and for some regions (Kamchatka, Central America, Japan - Sea of Japan) all the epicenters of the TEQ were located within the one hundred kilometer zone and that about 68% of the total number of the TEQ were located even closer within the 50 km zone. It was shown that most of the tsunami sources in Central America were located near the coastlines. The MOD value for this Central America region is equal to 10 km, and for South America the MOD value is = 34 km.

The close proximity of the source of a potential tsunamigenic earthquake to the coast may give the impression of false tsunami warnings for such regions, since the magnitude of the event is the only criterion used in the evaluation of the potential tsunami hazard.

A statistical analysis of TEQ of tectonic origin shows that a significant part of these events occur on the continental shelf, on the shallow part of the ocean near the coast, and in regions located near island arcs and marginal seas. In such areas, a substantial amount of sediments accumulates (Lisitzin 2013). Thus, when a substantial earthquake strikes, an unstable accumulation of sediments on the continental slopes may cause a shift of large masses of sedimentary material, underwater landslides and in the generation of a catastrophic tsunami. Our study noted that after a strong tsunamigenic earthquake occurred, a second event in the same region after 0.5 - 1 year, did not generate as strong of a tsunami. This observation indicates the need for a more careful and detailed analysis of the physical parameters as the sources of the TEQ and the geological conditions of the source's development.

At the end of the last century (Burymskaja et al. 1981), it was suggested that the sources of the TEQ have a relatively low average speed of the rupture generation and the long duration of the amplification of the oscillation intensity in P-wave. This may cause the redistribution of the energy balance in the focus and gain share in the low-energy part of the spectrum.

The peculiarities of the TEQ occurrences which were indicated above, can lead to some conclusions about some of the features, which are inherent just to tsunamigenic events.

1. Catastrophic earthquakes in the ocean ( $M \geq 8.5$ ) are almost always accompanied by a tsunami (100%), while strong earthquakes ( $M \geq 7.5$ ) generate a tsunami in only 24% of the cases (for the Pacific region). Such a selective response to a mechanical perturbation of the ocean can be associated with a rare appearance of EQ with a predominance of low-frequency components in the signal, generating less energy density.

2. Also noted was the zonal structure of the alternation in tsunami activity. Latitudinal zones of high activity were interchanged with zones of weak activity. The peaks of activity emerged in different times for different latitudinal zones, and the activation periods varied from 20 to 50 years.

3. Observed regularities can be the basis for constructing a model of tsunami occurrence taking into account the spatial and temporal distribution of events. A verification of the model involving algorithms and subsequent analysis of results, allow formulating new approaches to forecasting catastrophic tsunamis.

Model development of the evolution of the tsunami sources in space and time and verification (specification) models using observational data, will allow to advancement in the understanding of the causes of catastrophic tsunamis.

## ACKNOWLEDGMENTS

This work was supported partly by the Russian Foundation for Basic Research (projects No. 10-05-00116a, 11-05-07016d, 12-05-10031k and 13-05-00060a). We are grateful to Mikhail Nosov, Mikhail Rodkin and Yegenio Chirkov for the creative discussions and fresh wording, and we also express many thanks to Alik Ismail-Zade for useful comments in statistic technique.

## REFERENCES

Burymaskaia, R.N., Levin, B.W., Soloviev, S.L. (1981) A Kinematic Criterion of Submarine Earthquake Tsunami-genity // Doklady Akademii Nauk SSSR. Vol. 261, № 6. P. 1325-1329.

Gusiakov V. K. (2011) Relationship of Tsunami Intensity to Source Earthquake Magnitude as Retrieved from Historical Data, Pure Appl. Geophys. (168) 2033–2041, DOI 10.1007/s00024-011-0286-2

Historical Tsunami Database for the World Ocean -2010, (HTDB/WLD 2010), <http://tsun.sccc.ru/nh/tsunami.php>

(ISC), International Seismological Catalogue:  
<http://www.isc.ac.uk/iscbulletin/search/catalogue/>.

Levin, B. W. and E. V. Sasorova. (2002) On the 6-Year Tsunami Periodicity in the Pacific. J. Izvestiya, Physics of the Solid Earth, Vol. 38, No. 12, p. 1030.

Levin B.W., Sasorova E.V. (2002) Spatial and temporal periodicity in the Pacific tsunami occurrence. 3-rd Biennial Workshop on Subduction Processes emphasizing the Kurile-Kamchatkan-Aleutian Arcs. Fairbanks, Alaska, USA, June.

Levin, B. W. and E. V. Sasorova. (2005) Detection of Nonrandom Component in the Earthquake Distribution between the Northern and the Southern Hemispheres: Observations and Modeling. Doklady Earth Sciences. Vol. 401, No 2, pp.288-291.

Levin, and E. V. Sasorova. (2010) General Regularities in the Distribution of Seismic Events on the Earth and on the Moon. Doklady Earth Sciences, DOI: 10.1134/S1028334X10090230, Vol. 434, Part. 1, pp. 1249–1252.

Levin B.W., Sasorova E.V. (2013) Tsunami and Great Earthquake Space-Time Periodicity: Comparative Analysis. International Tsunami Symposium. ITS2013. Gocek, Turkey; Rhodes, Greece, 25-28 September. P.31.

Lisitzin A.P. (2013) Marine Geology - 40 years of the conference. Geology of seas and oceans. Proceedings of the XX International Scientific Conference (School) of marine geology. Vol.1. Moscow, p.5-13 (in Russian).

NGDC/NOAA (2010), Historical Tsunami Database (2010), Web-version: [http://www.ngdc.noaa.gov/hazard/tsu\\_db.shtml](http://www.ngdc.noaa.gov/hazard/tsu_db.shtml).

Sasorova, E.V. and B.W. Levin. (2004) Spatial and temporal periodicity in the Pacific tsunami occurrence. Submarine Landslides and Tsunamis, NATO Science Series IV, Earth and Environment Science, p.43-50, Kluwer Academic Publishers.

Sasorova E.V., B.W. Levin, O.N. Emelyanova. (2006). Detection of the non-random component in the earthquake distribution between the Northern and Southern part of the Pacific: observation and modeling. Earthquake Prediction. Ed. S. Mukherjee. Brill. Leiden-Boston. P.1-8.

Sasorova E.V., Korovin M.E., Morozov V.E., and Savochkin P.V. (2008) On the Problem of Local Tsunamis and Possibilities of Their Warning. ISSN 0001-4370, Oceanology, , Vol. 48, No. 5, pp. 634–645.

Sasorova E.V., Levin B.W., and Rodkin M.V. (2013) A common feature in latitudinal dependence of different geophysical processes occurring on the rotating Earth. Adv. Geosci., 35, 15–21, doi:10.5194/adgeo-35-15-2013.USGS/NEIC <http://neic.usgs.gov>